Optic Radiations Microstructural Changes in Glaucoma and Association With Severity: A Study Using 3Tesla-Magnetic Resonance Diffusion Tensor Imaging

Laury Tellouck,[1–3] Muriel Durieux,[4] Pierrick Coupé,[5,6] Audrey Cougnard-Grégoire,[2,3] Joy Tellouck,[1] Thomas Tourdias,[2,4,7] Fanny Munsch,[4] Arnaud Garrigues,[1] Catherine Helmer,[2,3] Florence Malet,[8] Jean-François Dartigues,[2,3] Vincent Dousset,[2,4,7] Cécile Delcourt,[2,3] and Cédric Schweitzer[1–3]

[1]CHU de Bordeaux, Service d'Ophtalmologie, Bordeaux, France
[2]University of Bordeaux, Bordeaux, France
[3]INSERM, U1219-Bordeaux Population Health Research Center, Bordeaux, France
[4]CHU de Bordeaux, Service de Neuro-Imagerie, Bordeaux, France
[5]Université de Bordeaux, LaBRI, UMR 5800, PICTURA, Talence, France
[6]CNRS, LaBRI, UMR 5800, PICTURA, Talence, France
[7]INSERM, U1215, Neurocentre Magendie, Bordeaux, France
[8]Centre d'Ophtalmologie Point Vision, Bordeaux, France

Correspondence: Cécile Delcourt, Inserm U1219, ISPED, 146 rue Léo Saignat, 33076 Bordeaux Cedex, France;
cecile.delcourt@isped.fr.

Submitted: April 29, 2016
Accepted: October 20, 2016

Citation: Tellouck L, Durieux M, Coupé P, et al. Optic radiations microstructural changes in glaucoma and association with severity: a study using 3Tesla-magnetic resonance diffusion tensor imaging. *Invest Ophthalmol Vis Sci*. 2016;57:6539–6547. DOI:10.1167/iovs.16-19838

Purpose. To compare microstructural changes along the optical radiations and brain structure volumes between glaucoma and control subjects using in vivo magnetic resonance imaging and to analyze their association with severity of the disease.

Methods. A total of 50 open-angle glaucoma subjects and 50 healthy age- and sex-matched controls underwent detailed ophthalmologic examinations (including visual field testing [VF], funduscopy, and spectral-domain optical coherence tomography) as well as diffusion tensor imaging (DTI) using 3.0-Tesla magnetic resonance imaging. Fractional anisotropy (FA), mean diffusivity, radial diffusivity (RD), and axial diffusivity (AD) were quantified semiautomatically along the optical radiations. DTI parameters and volumes of specific brain structures were compared between cases and controls using conditional logistic regression. Association between DTI metrics and the severity of the disease was studied using linear mixed regression analyses.

Results. In glaucoma subjects, optic radiations FA was significantly lower (0.57 vs. 0.59; $P = 0.02$) and RD was significantly higher (52.78 10^{-5} mm^2/s vs. 49.74 10^{-5} mm^2/s; $P = 0.03$) than in controls. Optic radiations FA was significantly correlated with homolateral functional and structural damage of glaucoma (mean deviation of VF [$P = 0.03$], retinal nerve fiber layer thickness [$P = 0.03$], vertical cup to disc ratio [$P = 0.0007$]). Volume and DTI parameters of other brain structures (including hippocampus) were not significantly different between glaucoma patients and controls.

Conclusions. We evidenced microstructural modifications along visual pathways of glaucoma patients and these alterations were correlated with disease severity. The association of glaucoma with other neurodegenerative alterations would need further exploration and a prospective follow-up of our cohort of subjects. (ClinicalTrials.gov number, NCT01621841).

Keywords: glaucoma, fractional anisotropy, 3T MRI, optic radiations, DTI

Glaucoma affects 64 million people and is the first cause of irreversible blindness, worldwide.[1,2] It encompasses a group of disorders characterized by progressive degeneration of the optic nerve head, loss of retinal ganglion cells, and a corresponding pattern of visual field (VF) loss.[3] Primary open-angle glaucoma (POAG) is the predominant form of glaucoma in Western countries. Although some risk factors for POAG have been identified (high IOP, age, high myopia, ethnicity, and heredity), several aspects of its pathophysiology remain unclear. As the disease could affect intracerebral visual pathways in addition to optic nerve head degeneration, a neurodegenerative hypothesis raises concerns.[4,5]

Central visual pathway degeneration in glaucoma was first suggested in experimental and histologic studies, which have evidenced that glaucoma is not strictly limited to the optic nerve.[6,7] In an animal model of ocular hypertension, brain changes were observed in the lateral geniculate nucleus and superior colliculus, in parallel with retinal ganglion cell loss.[8] In another study, gray matter of glaucoma patients was reduced compared with healthy subjects, in the approximate retinal lesion projection zones in the visual cortex.[9] Moreover, a

clinicopathologic case in humans highlighted a neural degeneration in intracranial optic nerve, lateral geniculate nucleus, and visual cortex.[10] This paradigmatic shift is further supported by several other small-sized clinical studies using brain magnetic resonance imaging (MRI), showing reduced volume of all the visual pathways (optic tracts, optic chiasm, lateral geniculate nucleus, optic radiations) measured at 1.5T[11–13] or 3.0T field strength.[14,15]

Some other experimental studies may help understand the pathogenesis of the disease. Using in vivo MRI studies is a way to study metabolic and spatiotemporal changes in glaucoma.[16–18]

In addition, epidemiologic studies also have suggested that glaucoma might be associated with other neurodegenerative disorders, in particular Alzheimer's disease,[19,20] and a few studies have found a reduced volume of brain structures beyond the visual pathways, particularly in the hippocampus, which is well known to be affected in Alzheimer's disease.[14,21,22] These data have nevertheless been collected in patients with longstanding disease. Whether subtle alterations suggestive of associated neurodegenerative disease can be captured from the early stage of glaucoma, before atrophy, is unknown.

Recent improvements in neuroimaging techniques allow more accurate evaluation of brain structure volumes and intracerebral microstructural damage. By quantifying microscopic movements of water molecules, diffusion tensor imaging (DTI), a functional MRI technique, provides a sensitive evaluation of underlying brain microstructural changes even before atrophy.[23] Therefore, this technique appears particularly promising in the documentation of intracerebral damage in glaucoma. The most commonly assessed DTI parameters include fractional anisotropy (FA, which reflects the degree of cellular structural alignment within fiber tracts and the structural integrity of the fiber tracts) and mean diffusivity (MD, which measures the average motion of water molecules independently of fiber directionality).

Several case-control studies have already shown that FA of the optic radiations is decreased and MD increased in glaucoma patients,[24,25] and some others have suggested that these changes may be progressive with increasing axon loss of the optic nerve.[26] Whereas these studies provide new insights in the understanding of glaucoma disease, they were limited in sample size and mainly included advanced glaucoma patients.

Therefore, our study aimed at exploring the potential neurodegenerative hypothesis associated with glaucoma and whether subtle changes could be measurable at the early stage of the disease. Thus, we analyzed both the microstructural changes of the visual pathway, in relation to glaucoma severity, as well as changes beyond the visual pathway, particularly in regions affected in neurodegenerative pathologies.

Methods

Patient Population

This study is an observational case-control study performed at the University Hospital of Bordeaux. Fifty patients with POAG (20 men, 30 women, mean age 61.9 ± 6.9 years) and 50 age- and sex-matched controls (20 men, 30 women, mean age 61.9 ± 7.0 years) were prospectively included.

This research followed the tenets of the Declaration of Helsinki. Participants gave written consent for participation in the study. The design of this study was approved by the Ethical Committee of Bordeaux (Comité de Protection des Personnes Sud-Ouest et Outre-Mer III) in March 2012. This study was registered on http://clinicaltrials.gov/ (identifier NCT01621841).

Ophthalmologic Examination

All participants underwent a complete ophthalmic examination, including measurement of best-corrected visual acuity, IOP using Goldmann applanation tonometry, gonioscopy, slit-lamp biomicroscopy, and optic disc examination by funduscopy. Central corneal thickness and anterior chamber depth were assessed using interferometry (OCT Visante; Carl Zeiss Meditec, Inc., Dublin, CA, USA), and axial length measurement using IOL Master (Carl Zeiss Meditec, Inc.). All participants underwent VF testing (Octopus 101; Haag-Streit, Inc., Bern, Switzerland) and only reliable tests (false-positive errors <15%, false-negative errors <15%, loss fixations <20%) were included. In addition, visual fields (VFs) were reviewed and excluded in the presence of artifacts, such as eyelid or rim artifacts, fatigue effects, inattention, or inappropriate fixation.

A measurement of peripapillary retinal nerve fiber layer (RNFL) thickness was performed using spectral-domain optical coherence tomography (SD-OCT) (Cirrus; Carl Zeiss Meditec, Inc.). All images were acquired and reviewed by specially trained technicians of the study to control the quality of signal strength and accurate centration and segmentation of the RNFL circle scan acquisition. Signal strength lower than 6 or acquisitions with artifacts were excluded from the analysis.

Glaucoma subjects and controls received a questionnaire requesting for cardiovascular risk factors, familial history of glaucoma, ophthalmologic diseases and current medications. Each participant underwent Mini Mental State Examination (MMSE).[27]

Primary open-angle glaucoma was defined by the following criteria: the presence of glaucomatous optic neuropathy (defined as a loss of neuroretinal rim with a vertical cup to disc ratio [VCDR] of >0.7 or an intereye asymmetry of >0.2, with or without notching attributable to glaucoma) associated with compatible VF loss. This VF loss was defined as the presence of at least three contiguous nonedge test points within the same hemifield on the pattern deviation probability plot at $P < 0.05$, with at least 1 point $P < 0.01$, excluding points directly above and below the blind spot, and the presence of glaucomatous hemifield test results outside normal limits. Iridocorneal angle opening was graded 3 or 4 on gonioscopy using Schaeffer classification.

Controls were defined as normal optic disc without notching or abnormal thinning of the neuroretinal rim, no VF defects, IOP measurement less than 21 mm Hg, and no family history of glaucoma.

Exclusion criteria included any diseases that could affect the VF, secondary glaucoma including exfoliative and pigmentary glaucoma, diabetes mellitus, any neurologic or psychiatric disorders, and a score less than 26 on the MMSE for global cognition. We also excluded participants according to standard MRI exclusion criteria, such as claustrophobia, ferromagnetic implants or pacemakers, and inability to lie still for the MRI acquisition time.

Stage of severity of glaucoma was classified according to the Hodapp-Parrish-Anderson classification.[28] The different stages are as follows:

- Stage 0: no or minimal defect
- Stage 1: MD ≥ –6.0 dB (early defect)
- Stage 2: –12.0 ≤ MD ≤ –6.0 dB (moderate defect)
- Stage 3: –20 ≤ MD ≤ –12.0 dB (advanced defect)
- Stage 4: MD ≤ –20.0 dB (severe defect)
- Stage 5: end-stage disease

Magnetic Resonance Imaging Data Acquisition

Magnetic resonance imaging examinations were performed on a 3-T Discovery MR750w scanner (GE Medical Systems, Milwaukee, WI, USA) using a 32-channel phased array head coil within 30 days after the ophthalmologic examinations. The protocol included a DTI sequence to look for microstructural alterations along and beyond the optic radiations, and a three-dimensional (3D) T1-weighted imaging sequence to look for global or focal atrophy. The parameters of acquisitions were as follows. The DTI sequence consisted in dual echo-planar imaging: 40 axial slices; repetition time, 12000 ms; echo time, 100.9 ms; slice thickness, 3.5 mm; matrix, 160 × 160; field of view, 24 × 24 cm; b values, 0 and 1000 s/mm^2 applied in 32 noncollinear directions. The 3D-T1 was an inversion recovery gradient echo sequence: 288 slices; repetition time, 11.4 ms; echo time, 4.3 ms; inversion time, 400 ms; flip angle, 15°; slice thickness, 0.8 mm; matrix, 384 × 384; field of view, 25 × 25 cm.

Image Processing

Measurement of DTI Metrics Along the Optic Radiations. From the DTI data, the distortions induced by eddy currents were first corrected, then a diffusion tensor model was fitted at each voxel using Olea Sphere software (Olea Medical, La Ciotat, France) to generate FA maps and to investigate the microstructural integrity of the optic radiations. The optic radiations were identified using deterministic tractography between two seed-regions of interest (ROIs) over the proximal and distal optic radiations according to previously published method and landmarks.[29] The proximal ROI was placed near the lateral geniculate nuclei, whereas the distal ROI was placed just anterior to its termination in the visual cortex. Fiber tract propagation was terminated for FA less than 0.2 and angle less than 35° based on agreed-upon thresholds. Regions of interest were placed by a specialized neuroradiologist symetrically, based on color-coded FA maps and trace DTI images on the anterior and posterior part of the expected pathway of the optic radiations (green boxes on the Fig.). Fibers whose directions did not correspond to the optic radiations based on anatomic knowledge and DTI-derived atlas were excluded by adding additional ROIs and a logical "not" function[30] (red boxes on the Fig.). Only fibers that connected the anterior and posterior ROIs were selected for further analysis. The analysis was independently repeated for a subset of cases (n = 25 of the 100 cases) by a specialized ophthalmologist with an intergrader agreement of 0.88.

The median FA and its subcomponent (axial and radial diffusivity, AD and RD, respectively), as well as the MD were measured along the reconstructed optic radiations (green streamlines on the Fig.). Decreased FA and increased MD values are usually considered as a proxy of axonal disruption.[31]

None of the people participating in FA measurements had any access to the case/control status of the participants, nor to any other clinical data.

Magnetic Resonance Imaging Volumetric Measurements. For volumetric analyses, T1-weighted images were processed using the volBrain system (http://volbrain.upv.es). After denoising,[32] images were affine-registered[33] into the Montreal Neurological Institute (MNI) space and the total brain volume was estimated using the Nonlocal Intracranial Cavity Extraction method.[34] Hippocampus was segmented using a patch-based multitemplate approach[35] following the international consortium from the European Alzheimer's Disease Consortium–Alzheimer's Disease Neuroimaging Initiative Harmonized Protocol for anatomical definitions of the hippocampus.[36] To control variations in head size between subjects, total brain volumes and hippocampal volumes were scaled using the volumetric scaling factor determined through the affine registration to the MNI brain template.

For DTI analysis within the hippocampus masks, an in-house pipeline (dtiBrain) was used to process diffusion-weighted images. First, diffusion-weighted images were affine-registered to the T1-weighted MRI in the MNI space.[32] Then, to compensate for echo-planar imaging distortion, a nonrigid registration was performed. Finally, a diffusion tensor model was fitted at each voxel using FSL 5.031 (fmrib.ox.ac.uk/fsl), generating FA and MD maps. Mean FA and MD were measured within the hippocampal masks previously generated on anatomical T1-weighted MRI.

Statistical Analysis

Statistical analysis was performed using SAS 9.3 (SAS Institute, Inc., Cary, NC, USA).

Differences of MRI characteristics between glaucoma subjects and healthy controls were tested using logistic conditional models, for parameters both along optic radiations and outside the visual pathway (globally for white and gray matter and in hippocampal and amygdala structures). Additionally, within the group of patients with glaucoma, we used mixed linear regression analyses, adjusted for sex and age (as a continuous variable expressed in years), to test the associations between optic radiation DTI parameters (FA, MD, AD, RD) and the parameters of severity of the disease (VCDR, mean deviation of VF and RNFL). This type of analysis allows taking into account both right and left sides of each patient, while taking into account the intraindividual correlation between sides. In particular, this allowed studying the associations of ocular parameters with homolateral (right optic radiation with right eye and left with left eye) and contralateral (right optic radiation with left eye and vice versa) optic radiations MRI parameters. In these regression analyses, both ocular and brain parameters were entered as z-scores. In addition, for RNFL, we also adjusted for axial length, which is strongly associated with RNFL.[37]

Results

Demographic and Ophthalmologic Characteristics

As shown in Table 1, cases and controls were similar for age, sex, history of cardiovascular diseases or risk factors, and MMSE. Family history of glaucoma was reported by 58% of glaucoma patients, and 0% of controls (because this was an exclusion criterion for controls).

As shown in Table 2, cases and controls did not significantly differ for visual acuity (distance and near), IOP, and axial length. As expected, they were significantly different for central corneal thickness, VCDR, RNFL thickness, and VF parameters. Similar results were observed for the left eye (Table 3).

In our study, 70% of glaucoma patients had an early stage of the disease, 20% a moderate stage, and 10% an advanced or severe stage, according to the Hodapp-Parrish-Anderson classification.

Comparison of MRI Parameters Along Optic Radiations Between Glaucoma and Control Subjects

One patient refused an MRI examination and three MRI examinations were of insufficient quality for analysis, leaving 49 glaucoma patients and 47 controls for the comparison of

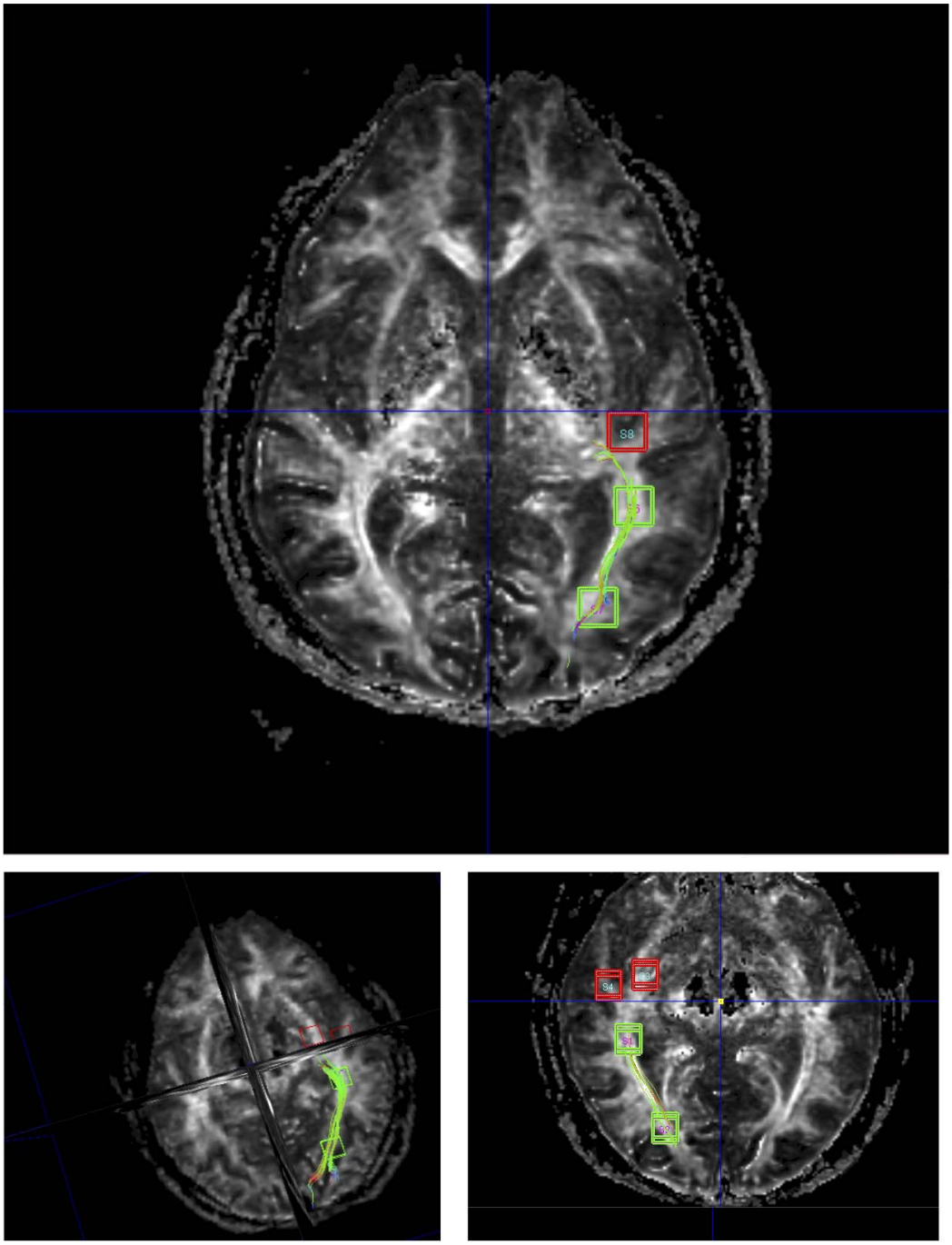

FIGURE. Building of optic radiations and measurement of fractional anisotropy, using the Olea Medical software (image: CHU de Bordeaux, Department of Neuroimaging). *Green boxes* are the markers placed manually on anterior and posterior parts of the optic radiations. *Green lines* are optic radiations automatically reconstructed by the Olea Medical software. *Red boxes* are markers placed manually to delete fibers outside the expected area.

MRI parameters (Table 4). The optic radiations were similarly reconstructed for glaucoma and control subjects (similar length and volume and reconstructed streamlines). Glaucoma patients showed significantly lower FA along the optic radiations than controls (0.57 vs. 0.59, $P = 0.02$), which was driven by significant increase in radial diffusivity (RD) (52.8 10^{-5} mm^2/s vs. 49.7 10^{-5} mm^2/s, $P = 0.03$), whereas axial diffusivity (AD) was unchanged. Mean diffusivity tended to be slightly higher in glaucoma patients, but this did not reach statistical significance (82.4 10^{-5} mm^2/s vs. 80.6 10^{-5} mm^2/s, $P = 0.10$).

Associations of Homo- and Contralateral Optic Radiation Parameters With the Severity of the Disease in Glaucoma Patients

Table 5 shows the associations of optic radiation parameters (FA, MD, RD and AD) with the ophthalmologic parameters of glaucoma severity evaluated by VF, optic disc cupping, and

Table 1. General Characteristics

Characteristics	Glaucoma, $n = 50$	Control, $n = 50$	P^*
Age, y, mean (SD)	61.9 (6.9)	61.9 (7.0)	0.98
Sex, *n*, (%)			1
Male	20 (40)	20 (40)	
Female	30 (60)	30 (60)	
MMSE, mean (SD)	29.3 (0.8)	29.4 (0.8)	0.7
Family history of glaucoma, *n* (%)			<0.0001
Yes	29 (58)	0 (0)	
No	16 (32)	50 (100)	
Unknown	5 (10)	0 (0)	
Self-reported medical history			
Hypertension, *n* (%)	11 (22)	12 (24)	0.81
Hypercholesterolemia, *n* (%)	14 (28)	12 (24)	0.65
Hypertriglyceridemia, *n* (%)	2 (4)	3 (6)	0.65
Myocardial infarction, *n* (%)	2 (4)	1 (2)	0.56
Smoking, *n* (%)			0.67
Never	29 (58)	25 (50)	
Former	17 (34)	19 (38)	
Current	4 (8)	6 (12)	

* χ^2 for categorical variables and Student's *t*-test for continuous variables.

RNFL thickness, only among patients with glaucoma ($n = 50$). We tested associations of ophthalmologic parameters with MRI parameters on the homolateral (right eye – right optic radiation and left eye – left optic radiation) and contralateral (right-left and left-right) sides. For the homolateral side, significant associations were found between optic radiations FA and mean deviation of the VF ($\beta = -0.22$; $P = 0.03$), VCDR ($\beta = -0.42$; $P = 0.0003$), and RNFL ($\beta = 0.22$; $P = 0.03$). The direction of the association is opposite for RNFL, because RNFL decreases with higher severity of glaucoma, whereas other parameters increase with severity. Mean and radial diffusivities increased with the severity of the disease measured by VCDR ($P < 0.006$ and $P < 0.0008$, respectively), but were not significantly associated with mean deviation of VF or RNFL thickness. By contrast, AD, as well as length and volume of optic radiations were not significantly associated with any of the severity parameters.

Table 2. Ophthalmologic Characteristics; Right Eye, Mean (SD)

Characteristics	Glaucoma, $n = 50$	Control, $n = 50$	P^*
Best-corrected visual acuity, logMAR			
Distance	0.03 (0.09)	0.006 (0.02)	0.09
Near	0.19 (0.07)	0.18 (0.00)	0.2
Central corneal thickness, µm	525.9 (30.9)	544.0† (31.9)	0.005
Axial length, mm	24.1 (1.1)	23.7 (1.2)	0.15
IOP, mm Hg	14.6 (3.7)	14.7 (2.5)	0.82
VCDR	0.8 (0.2)†	0.3 (0.2)†	<0.0001
RNFL thickness, µm	76.9 (17.7)	93.2 (9.9)	<0.0001
VF, dB			
Mean sensitivity	21.9 (6.1)	26.6 (1.1)	<0.0001
Mean deviation	5.0 (6.0)	0.3 (1.0)	<0.0001
Loss variance	22.6 (26.3)	5.0 (1.8)	<0.0001

* χ^2 for categorical variables and Student's *t*-test for continuous variables.

† One missing data point.

Table 3. Ophthalmologic Characteristics; Left Eye, Mean (SD)

Characteristics	Glaucoma, $n = 50$	Control, $n = 50$	P^*
Best-corrected visual acuity, logMAR			
Far	0.03 (0.08)	0.006 (0.02)	0.08
Near	0.2 (0.1)	0.2 (0)	0.1
Central corneal thickness, µm	524.6 (30.0)†	542.9 (28.4)‡	0.003
Axial length, mm	24.0 (1.0)	23.5 (0.8)	0.003
IOP, mm Hg	14.2 (3.2)	15.2 (2.4)	0.09
VCDR			
Funduscopy	0.8 (0.2)	0.3 (0.2)	<0.0001
RNFL thickness, µm	70.1 (18.7)	93.1 (9.7)	<0.0001
VF, dB			
Mean sensitivity	21.8 (4.6)	26.6 (1.2)	<0.0001
Mean deviation	5.1 (4.5)	0.3 (1.1)	<0.0001
Loss variance	28.1 (28.0)	4.7 (2.2)	<0.0001

* χ^2 for categorical variables and Student's *t*-test for continuous variables.

† One missing data point.

‡ Two missing data points.

With regard to the contralateral side, associations of MRI parameters with glaucoma severity parameters were much weaker, and reached statistical significance only for the association of FA and RD with VCDR ($P = 0.01$ and $P = 0.02$, respectively).

Brain Volume Analyses Between Cases and Controls

Finally, we did not evidence any statistically significant difference between glaucoma subjects and controls for volumes and DTI parameters of cerebrum white and gray matters, hippocampus, and amygdala (Table 6).

Discussion

Our study demonstrates microstructural changes of the optic radiations in glaucoma, as evaluated by lower FA driven by higher RD, and a correlation between the level of structural modifications and disease severity.

Using MRI at 1.5T[38] or 3.0T,[25,26,39] a few case-control studies also have reported such modifications of diffusion parameters in optic radiations of glaucoma patients. All these studies found significantly lower FA in glaucoma patients compared with control patients. In the present study, which included 70% of early stages of glaucoma, FA differences between cases and controls are numerically small (approxi-

Table 4. Comparison of MRI Parameters Along Optic Radiations Between Glaucoma and Control Subjects, Mean (SD)

MRI Parameters	Glaucoma, $n = 49$	Control, $n = 47$	P^*
FA	0.57 (0.04)	0.59 (0.03)	0.02
MD, 10^{-5} mm²/s	82.38 (6.43)	80.62 (4.87)	0.10
AD, 10^{-5} mm²/s	141.59 (7.14)	142.37 (6.74)	0.53
RD, 10^{-5} mm²/s	52.78 (6.74)	49.74 (5.04)	0.03
Length, mm	63.91 (6.80)	63.72 (7.15)	0.74
Volume, cm³	20.79 (9.13)	24.96 (12.33)	0.11

* *P* value: logistic conditional analyses.

Table 5. Associations of Homo- and Contralateral Optic Radiation Parameters With the Severity of the Disease in Glaucoma Patients

MRI Parameters	VF Mean Deviation		Funduscopy VCDR		SD-OCT Examination RNFL Thickness	
	β [95% CI]	*P*	β [95% CI]	*P*	β [95% CI]	*P*
Homolateral						
FA	−0.22 [−0.41 to −0.02]	**0.03**	−0.42 [−0.64 to −0.21]	**0.0003**	0.22 [0.03 to 0.41]	**0.03**
MD	0.02 [−0.17 to 0.21]	0.80	0.29 [0.08 to 0.50]	**0.008**	−0.15 [−0.34 to 0.04]	0.12
AD	−0.11 [−0.31 to 0.08]	0.26	0.09 [−0.14 to 0.31]	0.45	−0.06 [−0.26 to 0.14]	0.56
RD	0.09 [−0.10 to 0.28]	0.33	0.38 [0.17 to 0.59]	**0.0006**	−0.18 [−0.37 to −0.007]	0.06
Contralateral						
FA	−0.17 [−0.37 to 0.02]	0.09	−0.28 [−0.55 to −0.06]	**0.01**	0.10 [−0.09 to 0.30]	0.30
MD	0.13 [−0.06 to 0.31]	0.19	0.20 [−0.02 to 0.41]	0.07	0.01 [−0.18 to 0.21]	0.91
AD	0.04 [−0.15 to 0.24]	0.67	0.07 [−0.16 to 0.30]	0.55	0.09 [−0.11 to 0.30]	0.34
RD	0.15 [−0.04 to 0.34]	0.11	0.25 [0.04 to 0.46]	**0.02**	−0.03 [−0.23 to 0.16]	0.72

P value adjusted for age and sex, with additional adjustment for axial length for RNFL. Bold numbers indicate significant *P* values. CI, confidence interval.

mately 0.02 for a mean of approximately 0.60; i.e., approximately 3.3%). However, the SD is also small (approximately 0.04), showing low interindividual variability in this parameter, and the difference is substantial when related to the SD (approximately 0.5 SD), suggesting a major effect of glaucoma on this highly conserved parameter. In other studies, the differences in FA of optic radiations observed between glaucoma patients and controls were larger, but these studies generally included more severe cases. The study by Engelhorn et al.[39] included 22 severe glaucoma cases, and observed a difference in FA of optic radiations ranging from 17% to 30% according to the localization (anterior, central, posterior). The study by Murai et al.[38] included 18 severe glaucoma cases, 9 moderate and only 2 mild, and observed a 14% difference in FA of the optic radiations. The study by Garaci et al.[25] included four pre-perimetric glaucoma cases, four early, four moderate, and four severe cases, and observed a 36% difference in FA of the optic radiations. Finally, the study by Chen et al.[26] included mostly severe cases (36 of 50 eyes with MD >9.5 dB), but did not report numerically the averages of optic radiations FA.

Furthermore, we observed higher RD value in glaucoma patients and its correlation with disease severity, whereas AD was not significantly different between glaucoma and control patients. Although AD and RD are the two components of FA, these parameters have been scarcely analyzed in the literature, and some studies have already reported increasing RD in glaucoma subjects compared with controls.[24]

Even though the underlying pathologic alterations are not specifically known, animal studies have suggested that higher RD could mainly represent myelin loss, whereas lower AD could be a more specific marker of neuronal loss. However, these considerations were based on simplistic models and whether alterations of optic radiations truly predominate on myelin or axon component cannot be formally ascertained for glaucoma patients, for whom other modifications, such as microglia activation, may confound the data.

Additionally, we observed a trend toward higher MD value in the glaucoma group without reaching statistical significance. However, we observed a significant positive correlation between MD and disease severity measured with VCDR. Two studies also showed higher MD in glaucoma patients.[25,26] Although FA measures the degree of cellular structural alignment within fiber tracts and their structural integrity, MD measures the average motion of water molecules independently of fiber directionality and is considered as an additional marker of axonal disruption. As these studies included patients with advanced glaucoma, our findings might be explained by a lack of statistical power and a lower grade of disease severity in our glaucoma group. Such converging evidence of loss of fiber integrity in optic radiations in glaucoma cannot be measured in terms of length and volume of the optic radiations, which were similar in both groups, probably because our measurements were made before fiber loss or major disorganization.

We also observed an association of diffusivity parameters (mainly FA and RD), with the severity of glaucoma (assessed by mean deviation of the VF, VCDR and RNFL measured with SD-OCT), suggesting that microstructural changes to the optic radiations is one of the components of the severity that could participate in the clinical status of the patients and the alteration of the VF. Although we mainly included early and moderate glaucoma as defined by the Hodapp-Parrish-Anderson classification, our findings are consistent with some previous studies, which included more advanced cases.[26,38–40] All these studies also evidenced significant associations of optic radiations FA with structural parameters of optic nerve head degeneration evaluated with VCDR or time-domain RNFL thickness, as well as functional visual field alterations. For example, Michelson et al.[40] found a correlation between FA and VF. Thus, all these results illustrate the fact that FA could be a strong biomarker of glaucoma severity.

Our study also assessed the associations of glaucoma severity according to FA of homolateral and contralateral optic radiations. Interestingly, glaucoma severity parameters, in particular VCDR, were more strongly associated with homolateral optic radiations diffusion parameters than with contralateral parameters. As chiasmatic decussation of optic pathways results in approximately 50% crossing of axons on the contralateral side,[41] we would expect similar associations of glaucoma severity parameters with homolateral and contralateral diffusion parameters. However, our findings also might be related to an increased vulnerability of some specific retinal nerve fiber bundles of the optic nerve head resulting in an atrophy of optic radiations more predominant on the homolateral side of the decussation than on the contralateral. Indeed, several studies have demonstrated a specific vulnerability of the temporal and temporal-inferior sides of the optic nerve head to glaucoma damage.[42–44] Thus, we could expect an increased atrophy of the corresponding optic radiation predominant on the homolateral side that could explain our findings. However, even if temporal and temporal-inferior nerve fiber layers are more vulnerable to glaucomatous damage, the meaning of our findings should be interpreted with caution and would need further exploration to be confirmed and to identify the exact underlying mechanism. Indeed, distribution of RNFL is not homogeneous around the

Investigative Ophthalmology & Visual Science

TABLE 6. Comparison of DTI Parameters and MRI-Based Volume Between Glaucoma and Control Subjects, Mean (SD)

	Cerebrum White Matter			Cerebrum Gray Matter			Hippocampus			Amygdala		
MIR Parameters	Glaucoma, $n = 48$	Control, $n = 48$	P^*	Glaucoma, $n = 48$	Control, $n = 48$	P	Glaucoma, $n = 48$	Control, $n = 48$	P	Glaucoma, $n = 48$	Control, $n = 48$	P
Volume, cm^3	275.28 (115.61)	238.25 (59.03)	0.06	270.19 (59.03)	283.09 (38.17)	0.18	3.95 (0.53)	3.84 (0.46)	0.16	0.60 (0.23)	0.55 (0.18)	0.22
DTI parameters	$n = 41$	$n = 41$		$n = 41$	$n = 41$		$n = 41$	$n = 41$		$n = 41$	$n = 41$	
FA	0.38 (0.02)	0.37 (0.02)	0.39	0.17 (0.01)	0.17 (0.01)	0.45	0.19 (0.01)	0.19 (0.02)	0.44	0.15 (0.02)	0.15 (0.01)	0.09
MD, 10^{-5} mm^2/s	78.34 (3.58)	78.19 (3.21)	0.79	121.70 (9.63)	120.01 (8.81)	0.25	98.83 (8.82)	97.72 (5.79)	0.42	80.45 (4.03)	80.56 (3.40)	0.87
AD, 10^{-5} mm^2/s	110.91 (2.80)	110.35 (2.53)	0.26	138.84 (10.50)	136.96 (9.67)	0.24	116.86 (9.78)	115.46 (6.17)	0.39	92.64 (4.43)	92.21 (3.31)	0.57
RD, 10^{-5} mm^2/s	62.24 (4.17)	62.27 (3.78)	0.96	113.20 (9.23)	111.60 (8.44)	0.26	90.02 (8.40)	88.90 (5.74)	0.44	74.35 (3.99)	74.73 (3.53)	0.57

* P value: logistic conditional analyses.

optic nerve head with superior and inferior sectorial RNFL thicker than nasal or temporal RNFL sectors. Furthermore, the mean optic disc-fovea angle delimitating superior and inferior nerve fiber layers, is approximately 8°.[45] Thus, the exact distribution of nerve fiber layers of the retina that decussates to the contralateral optic tract or remains on the ipsilateral optic tract and finally leads to a vertical delimitation through the fovea on the hemivisual field test remains unclear. Hence, in our study, the corresponding optic radiations in the homo- or contralateral side could not be accurately matched to specific sectors of the retina or the optic nerve head.

Although high IOP is the main risk factor of glaucoma, this disease is increasingly considered as a neuro-ophthalmologic and neurodegenerative disease.[46] Furthermore, there are still controversies on the association between glaucoma and some other neurodegenerative diseases, such as Alzheimer's disease. In particular, in a cohort of elderly subjects followed every 2 years, we observed an association of POAG with incident dementia.[19] Volume changes beyond the visual system in glaucoma patients also have been reported in several studies but with inconsistent results. For instance, Frezzotti et al.[21] reported that POAG patients had brain atrophy in some gray matter regions and the visual cortex. By contrast, Williams et al.[22] found five cerebral structures larger in the glaucoma group than in the control group. Chen et al.[14] revealed both a decreasing gray matter volume in some regions and an increasing gray matter volume in some others. In the present study, we analyzed brain globally and focused on brain regions that are well known to be affected in the course of Alzheimer's disease, particularly hippocampus, and did not evidence any significant difference for any of the studied ROIs, neither in volume nor in parameters of diffusivity. However, as we included subjects with MMSE of 26 or more at baseline, the risk of brain structures atrophy was probably limited. Regarding the hippocampus, results have been particularly inconsistent, since Frezzotti et al.[21] reported decreased hippocampus volume in glaucoma patients, and Williams et al.[22] reported no significant difference of hippocampus volume between glaucoma and controls, but an increase in hippocampus volume with disease severity in patients with glaucoma.

Such differences between study results may be explained by differences in study methodology, in particular regarding the selection of subjects and severity of the disease, MRI sequences used, or definition of ROIs. For instance, in a recent study by Frezzotti et al.,[21] only severe cases of glaucoma (but not early) showed gray matter atrophy of the visual cortex and hippocampus.[47] The evolution of brain volume in the course of glaucoma and its association with other neurodegenerative diseases would need further investigation and prospective follow-up of subjects. Finally, functional MRI may offer new insights into the brain modifications associated with glaucoma, as suggested by two recent studies, showing functional modifications of the visual cortex at the earliest stages of the disease.[47,48]

In conclusion, we confirmed microstructural changes of optic radiations in glaucoma and its association with glaucoma severity. In accordance with several other studies, DTI appears as an objective measurement for evaluating alterations of the visual pathways in glaucoma and provides new insight in the pathophysiological process of glaucoma. A prospective evaluation of our cohort of patients would be of interest to observe the evolution of these microstructural modifications of optic radiations and to analyze the evolution of brain volume in association with the evolution of glaucoma disease. Diffusion tensor imaging could represent a future way to explore the central nervous system of glaucomatous subjects, leading to a better understanding of the pathophysiology and, potentially,

to help clinical trials evaluate new therapeutic strategies based on neuroprotection or brain repair.

Acknowledgments

Supported by Union Nationale des Aveugles et Déficients Visuels (UNADEV) (Bordeaux, France). Union Nationale des Aveugles et Déficients Visuels did not participate in the design of the study, the collection, management, statistical analysis, and interpretation of the data, nor in the preparation, review, or approval of the present manuscript.

Disclosure: **L. Tellouck**, Alcon (R), Allergan (R); **M. Durieux**, Bracco (R), Guerbet (R), Merck (R); **P. Coupé**, None; **A. Cougnard-Grégoire**, Laboratories Théa (R); **J. Tellouck**, None; **T. Tourdias**, None; **F. Munsch**, None; **A. Garrigues**, None; **C. Helmer**, Novartis (C); **F. Malet**, None; **J.-F. Dartigues**, Ispen, (F), Roche (F); **V. Dousset**, None; **C. Delcourt**, Allergan (C), Bausch & Lomb (C), Laboratories Théa (C, F, R), Novartis (C), Roche (C); **C. Schweitzer**, Alcon (C), Allergan (C), Laboratories Théa (C)

References

1. Resnikoff S, Pascolini D, Etya'ale D, et al. Global data on visual impairment in the year 2002. *Bull World Health Organ*. 2004; 82:844–851.
2. Tham Y-C, Li X, Wong TY, Quigley HA, Aung T, Cheng C-Y. Global prevalence of glaucoma and projections of glaucoma burden through 2040: a systematic review and meta-analysis. *Ophthalmology*. 2014;121:2081–2090.
3. Weinreb RN, Khaw PT. Primary open-angle glaucoma. *Lancet*. 2004;363:1711–1720.
4. O'Hare F, Rance G, McKendrick AM, Crowston JG. Is primary open-angle glaucoma part of a generalized sensory neurodegeneration? A review of the evidence. *Clin Experiment Ophthalmol*. 2012;40:895–905.
5. Gupta N, Yücel YH. Glaucoma as a neurodegenerative disease. *Curr Opin Ophthalmol*. 2007;18:110–114.
6. Yucel YH, Gupta N. A framework to explore the visual brain in glaucoma with lessons from models and man. *Exp Eye Res*. 2015;141:171–178.
7. Yücel Y. Central nervous system changes in glaucoma. *J Glaucoma*. 2013;22:S24–S25.
8. Zhang S, Wang H, Lu Q, et al. Detection of early neuron degeneration and accompanying glial responses in the visual pathway in a rat model of acute intraocular hypertension. *Brain Res*. 2009;1303:131–143.
9. Boucard CC, Hernowo AT, Maguire RP, et al. Changes in cortical grey matter density associated with long-standing retinal visual field defects. *Brain J Neurol*. 2009;132:1898–1906.
10. Gupta N, Ang L-C, Noël de Tilly L, Bidaisee L, Yücel YH. Human glaucoma and neural degeneration in intracranial optic nerve, lateral geniculate nucleus, and visual cortex. *Br J Ophthalmol*. 2006;90:674–678.
11. Gupta N, Greenberg G, de Tilly LN, Gray B, Polemidiotis M, Yücel YH. Atrophy of the lateral geniculate nucleus in human glaucoma detected by magnetic resonance imaging. *Br J Ophthalmol*. 2009;93:56–60.
12. Zhang YQ, Li J, Xu L, et al. Anterior visual pathway assessment by magnetic resonance imaging in normal-pressure glaucoma. *Acta Ophthalmol (Copenh)*. 2012;90:e295–e302.
13. Zikou AK, Kitsos G, Tzarouchi LC, Astrakas L, Alexiou GA, Argyropoulou MI. Voxel-based morphometry and diffusion tensor imaging of the optic pathway in primary open-angle glaucoma: a preliminary study. *AJNR Am J Neuroradiol*. 2012; 33:128–134.
14. Chen WW, Wang N, Cai S, et al. Structural brain abnormalities in patients with primary open-angle glaucoma: a study with 3T MR imaging. *Investig Opthalmology Vis Sci*. 2013;54:545.
15. Dai H, Mu KT, Qi JP, et al. Assessment of lateral geniculate nucleus atrophy with 3T MR imaging and correlation with clinical stage of glaucoma. *AJNR Am J Neuroradiol*. 2011;32: 1347–1353.
16. Chan KC, Fu Q, Hui ES, So K, Wu EX. Evaluation of the retina and optic nerve in a rat model of chronic glaucoma using in vivo manganese-enhanced magnetic resonance imaging. *NeuroImage*. 2008;40:1166–1174.
17. Chan KC, So K, Wu EX. Proton magnetic resonance spectroscopy revealed choline reduction in the visual cortex in an experimental model of chronic glaucoma. *Exp Eye Res*. 2009;88:65–70.
18. Ho LC, Wang B, Conner IP, et al. In vivo evaluation of white matter integrity and anterograde transport in visual system after excitotoxic retinal injury with multimodal MRI and OCT. *Invest Ophthalmol Vis Sci*. 2015;56:3788–3800.
19. Helmer C, Malet F, Rougier M-B, et al. Is there a link between open-angle glaucoma and dementia? The Three-City-Alienor Cohort. *Ann Neurol*. 2013;74:171–179.
20. Lin I-C, Wang Y-H, Wang T-J, et al. Glaucoma, Alzheimer's disease, and Parkinson's disease: an 8-year population-based follow-up study. *PLoS One*. 2014;9:e108938.
21. Frezzotti P, Giorgio A, Motolese I, et al. Structural and functional brain changes beyond visual system in patients with advanced glaucoma. *PLoS One*. 2014;9:e105931.
22. Williams AL, Lackey J, Wizov SS, et al. Evidence for widespread structural brain changes in glaucoma: a preliminary voxel-based MRI study. *Invest Ophthalmol Vis Sci*. 2013;54:5880–5887.
23. Le Bihan D, Iima M. Diffusion magnetic resonance imaging: what water tells us about biological tissues. *PLoS Biol*. 2015; 13:e1002203.
24. El-Rafei A, Engelhorn T, Wärntges S, Dörfler A, Hornegger J, Michelson G. A framework for voxel-based morphometric analysis of the optic radiation using diffusion tensor imaging in glaucoma. *Magn Reson Imaging*. 2011;29:1076–1087.
25. Garaci FG, Bolacchi F, Cerulli A, et al. Optic nerve and optic radiation neurodegeneration in patients with glaucoma: in vivo analysis with 3-T diffusion-tensor MR imaging. *Radiology*. 2009;252:496–501.
26. Chen Z, Lin F, Wang J, et al. Diffusion tensor magnetic resonance imaging reveals visual pathway damage that correlates with clinical severity in glaucoma. *Clin Experiment Ophthalmol*. 2013;41:43–49.
27. Folstein MF, Folstein SE, McHugh PR. "Mini-mental state". A practical method for grading the cognitive state of patients for the clinician. *J Psychiatr Res*. 1975;12:189–198.
28. Maeda N, Klyce SD, Smolek MK, Thompson HW. Automated keratoconus screening with corneal topography analysis. *Invest Ophthalmol Vis Sci*. 1994;35:2749–2757.
29. Reich DS, Smith SA, Gordon-Lipkin EM, et al. Damage to the optic radiation in multiple sclerosis is associated with retinal injury and visual disability. *Arch Neurol*. 2009;66:998–1006.
30. Wakana S, Jiang H, Nagae-Poetscher LM, van Zijl PCM, Mori S. Fiber tract-based atlas of human white matter anatomy. *Radiology*. 2004;230:77–87.
31. Wheeler-Kingshott CA, Trip SA, Symms MR, Parker GJM, Barker GJ, Miller DH. In vivo diffusion tensor imaging of the human optic nerve: pilot study in normal controls. *Magn Reson Med*. 2006;56:446–451.
32. Manjón JV, Coupé P, Martí-Bonmatí L, Collins DL, Robles M. Adaptive non-local means denoising of MR images with spatially varying noise levels. *J Magn Reson Imaging*. 2010; 31:192–203.
33. Avants BB, Tustison NJ, Song G, Cook PA, Klein A, Gee JC. A reproducible evaluation of ANTs similarity metric performance in brain image registration. *NeuroImage*. 2011;54: 2033–2044.

Investigative Ophthalmology & Visual Science

34. Manjón JV, Eskildsen SF, Coupé P, Romero JE, Collins DL, Robles M. Nonlocal intracranial cavity extraction. *Int J Biomed Imaging*. 2014;2014:820205.
35. Coupé P, Manjón JV, Fonov V, Pruessner J, Robles M, Collins DL. Patch-based segmentation using expert priors: application to hippocampus and ventricle segmentation. *NeuroImage*. 2011;54:940–954.
36. Frisoni GB, Jack CR, Bocchetta M, et al. The EADC-ADNI Harmonized Protocol for manual hippocampal segmentation on magnetic resonance: evidence of validity. *Alzheimers Dement*. 2015;11:111–125.
37. Sowmya V, Venkataramanan VR, Prasad V. Effect of refractive status and axial length on peripapillary retinal nerve fibre layer thickness: an analysis using 3D OCT. *J Clin Diagn Res*. 2015;9: NC01–NC04.
38. Murai H, Suzuki Y, Kiyosawa M, Tokumaru AM, Ishii K, Mochizuki M. Positive correlation between the degree of visual field defect and optic radiation damage in glaucoma patients. *Jpn J Ophthalmol*. 2013;57:257–262.
39. Engelhorn T, Michelson G, Waerntges S, et al. A new approach to assess intracranial white matter abnormalities in glaucoma patients: changes of fractional anisotropy detected by 3T diffusion tensor imaging. *Acad Radiol*. 2012;19:485–488.
40. Michelson G, Engelhorn T, Wärntges S, El Rafei A, Hornegger J, Doerfler A. DTI parameters of axonal integrity and demyelination of the optic radiation correlate with glaucoma indices. *Graefes Arch Clin Exp Ophthalmol*. 2013;251:243–253.
41. Pietrasanta M, Restani L, Caleo M. The corpus callosum and the visual cortex: plasticity is a game for two. *Neural Plast*. 2012;2012:1–10.
42. Strouthidis NG, Fortune B, Yang H, Sigal IA, Burgoyne CF. Longitudinal change detected by spectral domain optical coherence tomography in the optic nerve head and peripapillary retina in experimental glaucoma. *Invest Ophthalmol Vis Sci*. 2011;52:1206–1219.
43. Tan O, Chopra V, Lu AT-H, et al. Detection of macular ganglion cell loss in glaucoma by Fourier-domain optical coherence tomography. *Ophthalmology*. 2009;116:2305–2314.e1 –e2.
44. Yang Y, Zhang H, Yan Y, Gui Y, Zhu T. Comparison of optic nerve morphology in eyes with glaucoma and eyes with non-arteritic anterior ischemic optic neuropathy by Fourier domain optical coherence tomography. *Exp Ther Med*. 2013; 6:268–274.
45. Jonas RA, Wang YX, Yang H, et al. Optic disc-fovea angle: the Beijing Eye Study 2011. *PLoS One*. 2015;10:e0141771.
46. Chang EE, Goldberg JL. Glaucoma 2.0: Neuroprotection, neuroregeneration, neuroenhancement. *Ophthalmology*. 2012;119:979–986.
47. Murphy MC, Conner IP, Teng CY, et al. Retinal structures and visual cortex activity are impaired prior to clinical vision loss in glaucoma. *Sci Rep*. 2016;6:31464.
48. Frezzotti P, Giorgio A, Toto F, De Leucio A, De Stefano N. Early changes of brain connectivity in primary open angle glaucoma [published online ahead of print August 9, 2016]. *Hum Brain Mapp*. doi:10.1002/hbm.23330.